


Investigation of photocatalytic performance of natural zeolite/TiO₂ composites

Hassan Koohestani , Mohammad Hassanabadi, Hamed Mansouri, Abbas Pirmoradian

Faculty of Materials and Metallurgical Engineering, Semnan University, Semnan, Iran

✉ E-mail: h.koohestani@semnan.ac.ir

Published in Micro & Nano Letters; Received on 7th December 2018; Revised on 3rd February 2019; Accepted on 25th February 2019

The growing increase of industrial wastewater, environmental contaminations, and the necessity of clean water has stressed the importance of removing pollutants. One of the effective means of removing pollutants from water and wastewater is by utilising zeolite. Zeolite, despite possessing unique photophysical properties (such as numerous fine cavities, the high capability to adsorb, and chemical–thermal stability), represents some limitations when being used. Depositing photocatalysts on zeolite particles to improve its removal potential is of much interest. In this work, therefore, TiO₂ nanoparticles were deposited on fine particles of zeolite. Zeolite/TiO₂ composites were evaluated by X-ray diffractometer, scanning electron microscope, Brunauer–Emmett–Teller, diffuse reflectance spectroscopy analyses. The results indicate that the presence of TiO₂ nanoparticles reduces the specific surface area. However, it causes the ability to absorb UV light. Increasing the amount of TiO₂ any further will bring about a redshift in absorption edge. Photocatalytic properties of the composites were assessed by methyl orange and cyanide ion removal examination. The 10%TiO₂ composite with the specific surface area of 34 m²/g and bandgap energy of 3.3 eV showed to be the most efficient. The superior photocatalytic performance of 10%TiO₂ sample was confirmed by the examination of producing hydrogen from water/methanol.

1. Introduction: The environment and the underground water resources are being contaminated at an accelerating rate by the industrial wastewaters discharged by rapid expansions of industries. Various contaminants including heavy metals and organic compounds are serious threats against living creatures, hence the essential of wastewater treatment [1–3]. Consequently, different approaches have been introduced including chemical distribution with hydroxide, sulphide and chemical deposits, ion exchange, adsorption by porous carbon materials, biosorbents, filtering by electrode membrane dialysis, coagulation, freezing, and flotation almost all of which have adverse side effects [2, 4, 5].

In the last three decades, new methods such as oxidation, and adsorbing the pollutants by zeolite and photocatalysts have been focused on owing to their low initial cost, the simplicity of design, ease of operation, and the possibility of reusing the resulted water [6, 7].

Zeolite is a microporous mineral mainly consisting of aluminosilicate having a large specific surface area, and high chemical and thermal stability [2, 3, 8]. Different types of natural and artificial zeolites are used in different researches. Among the various natural zeolites, however, only nine species predominate in nature. Natural zeolites divide into the three categories of string, column, and mixed in terms of their crystalline morphology. Physical and chemical properties of natural zeolites differ [9–11]. Moreover, different samples of a specific zeolite show dissimilarity in their physical properties (porosity size, crystal size, ion-exchange capacity, and adsorption capacity), and chemical composition [3, 7]. In addition to adsorbing impurities and treating water, the zeolite is used in medical and agricultural industries, and also garment detergents. However, zeolite efficiency in adsorbing and removing pollutants needs to be improved [10–12].

There has been an increasing tendency to use semiconducting photocatalysts recently [6, 11]. Photocatalysts are fundamentally based on electron–hole pair production in the semiconductor through adsorbing light whose bandgap is higher than or equal to that of the semiconductor [1, 13]. Such electron–holes are capable of reacting with the water molecules and the oxygen adsorbed on the semiconductor's surface, a process through which powerful radicals of hydroxyl (OH[•]) are formed leading to the decomposition of pollutants in the water [11, 14]. One of these semiconducting photocatalysts is titanium dioxide (TiO₂),

which is of much importance owing to possessing incomparable features of low cost, non-toxicity, and light and chemical stability [1, 4].

Depositing nanoparticles of TiO₂ on the surface of zeolite not only offers the remarkable absorbability of zeolite but also provides the exceptional ability of TiO₂ to degradation water pollutants [10, 12]. Many types of research have addressed their studies to amend artificial zeolite through the means of different photocatalysts in which the impact of various parameters upon zeolite's ability to adsorb and degradation pollutants has been investigated, and the optimum conditions have been presented [8, 11]. Nevertheless, there has been little research on amending natural zeolite by photocatalysts in general and by TiO₂ in particular [3].

Therefore, in this work, the natural zeolite is improved by TiO₂ nanoparticles, and its physicochemical properties are investigated using different analyses. Furthermore, utilising methyl orange (MeO) and cyanide ion removal, and hydrogen production examinations, the obtained samples will be assessed regarding their performance of adsorbing the pollutants and removing them.

2. Experimental

2.1. Materials: The natural zeolite of clinoptilolite + cristobalite + quartz with the composition presented in Table 1 was obtained from Afrazand-e Semnan Company. Titanium isopropoxide (TTIP), hydrochloric acid (HCl), isopropanol, MeO, and potassium cyanide were purchased from Merk Company.

2.2. Experimental procedure: To produce the composite of zeolite/TiO₂, TiO₂ nanoparticles were synthesised by using chemical methods as described in our previous work [1, 4]. In brief, 85 ml of ionised water, 6 ml of hydrochloric acid, and 6 ml of 2-propanol were stirred on a magnetic stirrer. Then 5 ml of titanium isopropoxide was dropped into the solution. Gradually, the solution's temperature was increased to 60°C in a water bath. After that, to obtain zeolite-based composites, a certain amount of zeolite powder, which was previously washed by ethanol and ionised water, and then dried, was added to the solution. The zeolite-based composites of 5, 10, 15, and 20% of TiO₂ were acquired and abbreviated as Z5T, Z10T, Z15T, and Z20T. Having been stirred for 1 h, the solution was then kept under room temperature for 24 h to have

Table 1 Chemical analysis of used natural zeolite

Components	SiO ₂	Al ₂ O ₃	Fe ₂ O ₃	CaO	Na ₂ O	K ₂ O
%wt	67.82	10.91	0.65	0.89	3.85	4.07

TiO₂ particles deposited on zeolite. Afterwards, the filtered deposit was dried at 80°C for 1 h, and calcined at 450°C for 2 h.

After each time of adsorbing the pollutants, to reuse the composite, it was washed for 10 h in water and dried at 80°C for 10 h.

2.3. Characterising zeolite/TiO₂ composite: The crystalline phases of the synthesised samples were examined using an X-ray diffractometer (XRD, Bruker D8, Germany) with monochromated Cu-K α radiation ($\lambda = 1.54056 \text{ \AA}$). Crystallite sizes of TiO₂ phases were calculated by Debye-Scherrer ($D = 0.89\lambda/\beta\cos\theta$). The morphology of the particles was analysed by scanning electron microscope (SEM, XL 30-Philips, the Netherlands). The Brunauer–Emmett–Teller (BET), -specific surface areas of the synthesised samples, were determined using a BET surface analyser (Belsorp mini II; Bel, Japan).

It is known that the photocatalytic performance of a material depends on its bandgap energy. Therefore, using BaSO₄ as a reference, the light absorption spectrum of the samples was measured at room temperature by a UV spectrophotometer (Avaspec-2048TEC, the Netherlands). Absorption onset wavelength (λ_g , nm) of the crossing point is between the line extrapolated from the onset of the rising part of the absorption spectrum and axis X of the curve. Bandgap (E_g , eV) was measured by the following equation [15]:

$$E_g = \frac{1243.1}{\lambda_g} \quad (1)$$

2.4. Photocatalytic performance of zeolite/TiO₂ composite: To investigation the photocatalytic performance of zeolite/TiO₂ composite, MeO and potassium cyanide (CN) were removed by the composite and the results were then compared. 50 ml solutions of MeO (with the initial concentration of 5 ppm) and CN (with the initial concentration of 50 ppm) were made. 1 g/l of the composite was applied to each solution then. The examination was carried out at a constant temperature. pH was specified for each solution (4.5 for MeO solution, and 10 for CN). Before radiation had started, each solution had been stirred in the dark for 1 h so as the solutions could reach their adsorption–desorption equilibrium. Subsequently, the system was placed under the UV light of two lamps (6 W lamp – Philips, China), the surfaces of solutions being 10 cm away from the lights. Throughout the examination, a sample of each solution was taken at 30 min intervals, and the concentration of the pollutant was determined utilising a UV–vis spectrophotometer device. The extent of the degradation was measured by the following equation:

$$\eta\% = \left(\frac{C_0 - C}{C_0} \right) \times 100 \quad (2)$$

where C_0 is the initial concentration of the pollutant in the solution, and C is that of the pollutant after the time t [15].

2.5. Photocatalytic production of hydrogen: To produce hydrogen, a 200 ml solution of water/methanol (50:50) was used in a 750 ml Pyrex reactor. Creating a vacuum, the space above the solution in the reactor was evacuated from any gases. Sampling was done every 30 min. The amount of the produced hydrogen was measured by TCD type gas chromatography (GC, model 2550TG, Islamic Republic of Iran).

3. Results and discussion: Fig. 1 illustrates the XRD pattern for the sample of natural zeolite and Z10T composite which was calcined for 2 h at 450°C. The peaks in Fig. 1a related to the constituents of natural zeolite, which three phases clinoptilolite, cristobalite, and quartz have been identified. In Fig. 1b, which is the pattern of the sample Z10T, in addition to different peaks of the composing constituents of zeolite, the peaks of TiO₂ were also identified. These peaks were at the angles of 25.6°, 37.8°, 47.9°, and 54.6° (anatase phase) and the angles of 27.5°, 36.3°, and 56.7° (rutile phase) [1, 6]. The intensity of the peaks for rutile in composites is relatively lower than rutile in pure TiO₂. The presence of zeolite delays the anatase to rutile phase transformation. This behaviour has been reported in similar studies [10, 16]. According to the Scherrer equation, the crystallite size of anatase and rutile were determined to be 23.2 and 26.4 nm, respectively.

The morphology of the natural zeolite and composite of Z10T samples can be seen in Fig. 2. Zeolite particles are non-uniform

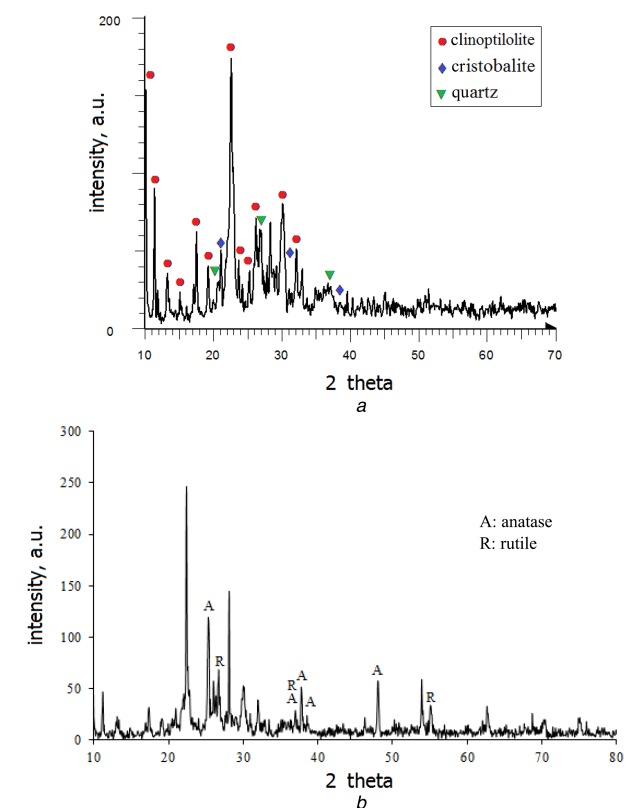


Fig. 1 XRD pattern
a Used natural zeolite
b Z10T composite

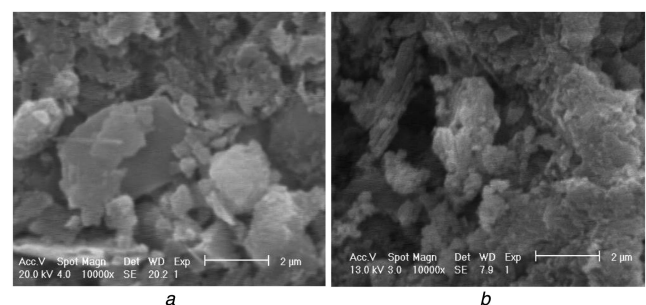


Fig. 2 SEM image
a Used natural zeolite and
b Zeolite/10%TiO₂ composite

and scale-like in shape falling in the approximate range of 0.2–3 μm . After the deposition of TiO_2 nanoparticles on natural zeolite, no remarkable change can be observed in the shape of the particles. However, zeolite particles are agglomerated after the deposition, hence the formation of larger masses. In other terms, the synthesis of TiO_2 causes a bond and joint among zeolite particles.

Specific surface areas of different samples are given in Table 2. As it can be evidenced the largest specific area belongs to natural zeolite (35 m^2/g) while it is decreased after TiO_2 deposition. As the amount of deposited TiO_2 rises, the surface area of the composite declines owing to the zeolite's surface cavities being filled. Furthermore, as illustrated in SEM images, synthesis of TiO_2 nanoparticles on zeolite particles results in their agglomeration and enlargement which leads to a decrease in the specific surface area. According to the previous research [4], pure TiO_2 with the size range of 20–40 nm has a specific surface area of 68 m^2/g . Sacco *et al.* [17] reported a decrease of the specific area from 52 to 24 m^2/g after the depositing ZnO nanoparticles on the zeolite.

Since the photocatalytic performance of a given material is heavily dependent on its optical properties, different samples were analysed regarding their optical properties, and their UV–vis diffuse reflectance spectrometry curves are presented in Fig. 3. The results of analysing the absorption curves are displayed in Table 2. It is apparent that pure zeolite has no absorption after 240 nm. Adding TiO_2 causes a move and red shift in the absorption edge of the sample. Absorption edge for TiO_2 has eventually occurred at 390 nm. On the other hand, adding greater amounts of TiO_2 to zeolite might widen the absorption edge of the sample. Comparing bandgap energy values of the different samples indicate that increasing the amount of TiO_2 is followed

by a decrease in the bandgap energy. So that the bandgap energy in the Z20 T is ~ 3.25 eV, which is still higher than that of pure TiO_2 (2.95 eV) synthesised under similar conditions [4]. When the TiO_2 is pure, the surface of the particles is not affected by any material (such as zeolite), and so the nanoparticles show their actual absorption edge.

To study the photocatalytic performance of zeolite/ TiO_2 composites, the extent to which the pollutants of MeO and CN ion could be degraded using the composites were compared. Figs. 4 and 5 show the efficiency of removing these pollutants by various zeolite/ TiO_2 composites under the radiation of UV light. It is evident that the efficiency of the composites is higher than that of pure zeolite and TiO_2 . This is due to benefiting from adsorption properties of zeolite and photocatalytic characteristics of TiO_2 both. However, different samples exhibited different capabilities to degradation MeO and CN ion. Such differences can be linked to surface charges of the particles.

Orange methyl is an anion colour and participates in the solution as negative ions [1]. Moreover, pH_{PZC} (point of zero charge) of zeolite/ TiO_2 composite is 5.9 [18]. Consequently, in the solution of MeO, ($\text{pH}=4.5$) the surface of the composite particles has positive charges. Ions of H^+ are attracted to atoms of nitrogen in the azo group of MeO. Therefore, a powerful electrostatic attraction will be formed between the surface of particles and MeO molecules [5, 19, 20].

The composite's surface, nevertheless, has negative charges for cyanide ion ($\text{pH}=10$) and as it can be observed, this electrostatic repulsion between the surface of particles and CN ion is responsible for a lower decomposition efficiency in comparison with that of MeO. It shall also be noted that for pH values lower than 8, hydrogen cyanide (HCN), which is highly hydrophilic and

Table 2 Surface area and optical properties of samples

Sample	Specific surface area, m^2/g	Absorption edge wavelength, nm	Bandgap, eV
Z	35	—	—
TiO_2	68 ^a	422	2.95 ^a
Z5T	32	335	3.72
Z10T	31	358	3.47
Z15T	28	373	3.33
Z20T	26	382	3.25

^aSee [1, 4].

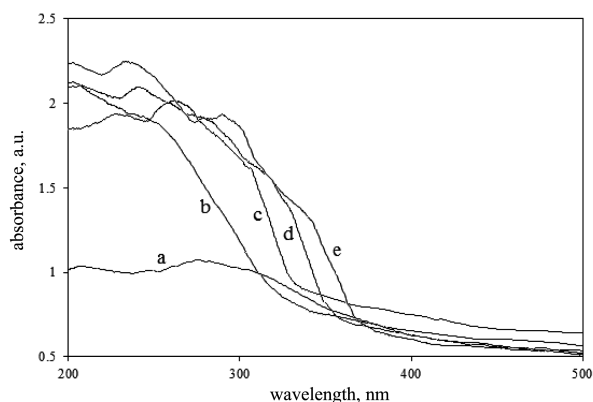


Fig. 3 Diffuse UV–vis absorbance spectra of
a Zeolite
b Z5T
c Z10T
d Z15T
e Z20T

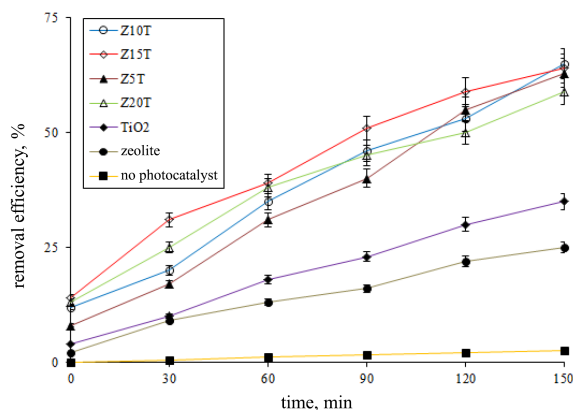


Fig. 4 Removal efficiency of MeO by different samples

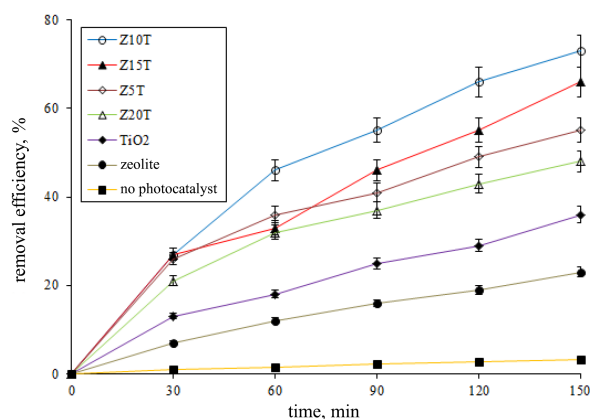


Fig. 5 Removal efficiency of cyanide by different samples

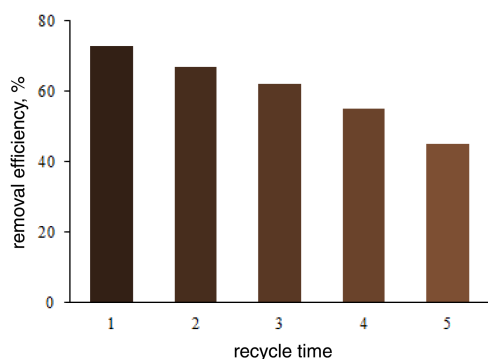


Fig. 6 Reusability of the Z10T for MeO degradation

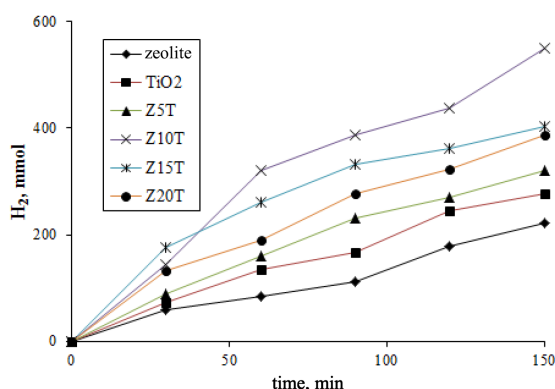
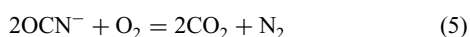
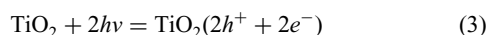


Fig. 7 H₂ generation by used composites from 50 vol.% methanol solution

poisonous gas, will be generated and this can cause environmental pollution [19]. Hence decomposing cyanide ion was carried out in pH values over 10. The chemical reactions governing removing and decomposing cyanide ion by TiO₂ are as follows [1, 4, 19]:

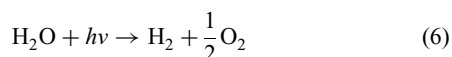


Additionally, anionic portions of cyanide are absorbed by cationic absorbing surfaces in the zeolite, and this improves the decomposition process by the composite [1].

The diagrams in Figs. 4 and 5, nonetheless, illustrate that different ZT composites are of different capabilities to remove MeO and CN. Maximum efficiency in removing the pollutants belongs to Z10T, which is 73% for MeO, and 65% for CN.

Reusability of Z10T composite in removing the dye of MeO was also studied. Fig. 6 portrays the photocatalytic performance of the composite having been reused for five times. As it can be predicted, the efficiency of the composite in removing the dye gradually lowers, dropping from 73 to 45% after five times' reuse. This reduction of efficiency can be related to dissolution and waste of TiO₂ particles after each time being used.

Fig. 7 depicts the photocatalytic production of hydrogen by ZT composites under UV light radiation. It is obvious that the amount of hydrogen produced by the composites is higher than when pure zeolite or TiO₂ is used. The photocatalytic reaction to produce hydrogen is as follows [21]:



Methanol has been utilised as a sacrificial electron donor to facilitate photoreduction. One of the challenges of employing photocatalysts is the high rate at which electron–holes formed by light are recombined before being used in oxidation–reduction reactions. Methanol reduces the rate of recombination by effectively separating the holes [21, 22].

Pairs of electron–holes are formed in TiO₂ nanoparticles of the ZT composites by the radiation of light, and zeolite, possessing distinctive photophysical properties such as controlling charge transfer and charge transfer processes, plays a crucial role in producing hydrogen. Furthermore, since cavities present in zeolite are very small in size, the solution and zeolite come into a greater contact. Thus, the reactions take place in a wider area because of the numerous active surface locations. The reduction in the rate of charge recombination is facilitated as well [21].

Nonetheless, an optimum amount of the photocatalyst of TiO₂ shall be used. In greater amounts cavities in zeolite will be occupied, and the specific surface area of the composite will reduce, and the amount of light reaching the composite will diminish, hence less hydrogen production. The results in the current study confirm such a reduction caused by excessive amounts of TiO₂. In this study, Z10T produced the highest amount of hydrogen (534 mmol) in comparison with other composites.

4. Conclusion: In this study, the nanoparticles of TiO₂ were deposited on natural zeolite successfully. Composites were characterised by XRD, SEM, BET, and DRS analyses. The presence of TiO₂ nanoparticles, despite reducing the specific surface area, causes a red shift in the absorption edge, and lowers its bandgap energy. Photocatalytic properties of the composites were examined by the efficiency of MeO and cyanide ion removal, and hydrogen production from water/methanol under UV light radiation. The results indicated that adding an optimum amount of TiO₂ on zeolite particles (10%wt) will lead to the best photocatalytic performance. Electron–hole formation in TiO₂, and zeolite's role in yielding a larger specific surface area and in reducing electron–hole recombination rate, improve the photocatalytic performance of ZT composites compared to those of zeolite or TiO₂ alone.

5. Acknowledgments: The authors thank the Afrazand-e Semnan Company for the supply of natural zeolite. They also appreciate Mr Rajabi for advice and guidance.

6 References

- [1] Koohestani H., Sadrnezhad S.K.: 'Photocatalytic degradation of methyl orange and cyanide by using TiO₂/CuO composite', *Desalination Water Treat.*, 2016, **57**, (46), pp. 22029–22038
- [2] Huang Y., Zeng X., Guo L., *ET AL.*: 'Heavy metal ion removal of wastewater by zeolite-imidazolate frameworks', *Separation. Purif. Technol.*, 2018, **194**, pp. 462–469
- [3] Zhang G., Song A., Duan Y., *ET AL.*: 'Enhanced photocatalytic activity of TiO₂/zeolite composite for abatement of pollutants', *Microporous Mesoporous Mater.*, 2018, **255**, pp. 61–68
- [4] Koohestani H., Sadrnezhad S.K.: 'Photocatalytic activity of immobilized geometries of TiO₂', *J. Mater. Eng. Perform.*, 2015, **24**, (7), pp. 2757–2763
- [5] Abidin A.Z., Abu Bakar N.H.H., Ng E.P., *ET AL.*: 'Rapid degradation of methyl orange by Ag doped zeolite X in the presence of borohydride', *J. Taibah Univ. Sci.*, 2017, **11**, (6), pp. 1070–1079
- [6] Koohestani H., Sadrnezhad S.K.: 'Improvement in TiO₂ photocatalytic performance by ZrO₂ nanocompositing and immobilizing', *Desalination Water Treat.*, 2016, **57**, (58), pp. 28450–28459
- [7] Malekian R., Abedi-Koupai J., Eslamian S.S., *ET AL.*: 'Ion-exchange process for ammonium removal and release using natural Iranian zeolite', *Appl. Clay Sci.*, 2011, **51**, (3), pp. 323–329
- [8] Liu R., Dangwal S., Shaik I., *ET AL.*: 'Hydrophilicity-controlled MFI-type zeolite-coated mesh for oil/water separation', *Separation Purif. Technol.*, 2018, **195**, pp. 163–169

- [9] Batistela V.R., Fogaça L.Z., Fávaro S.L., *ET AL.*: 'Zno supported on zeolites: photocatalyst design, microporosity and properties', *Colloid. Surf. A*, 2017, **513**, pp. 20–27
- [10] Guesh K., Márquez-Álvarez C., Chebude Y., *ET AL.*: 'Enhanced photocatalytic activity of supported TiO₂ by selective surface modification of zeolite Y', *Appl. Surf. Sci.*, 2016, **378**, pp. 473–478
- [11] Chen J., Eberlein L., Langford C.H.: 'Pathways of phenol and benzene photooxidation using TiO₂ supported on a zeolite', *J. Photochem. Photobio. A*, 2002, **148**, (1–3), pp. 183–189
- [12] Ichiura H., Kitaoka T., Tanaka H.: 'Removal of indoor pollutants under UV irradiation by a composite TiO₂-zeolite sheet prepared using a papermaking technique', *Chemosphere*, 2003, **50**, (1), pp. 79–83
- [13] Tatarchuk T., Peter A., AlNajar B., *ET AL.*: 'Photocatalysis: activity of nanomaterials', in Hussain C.M., Mishra A.K. (Eds.): 'Nanotechnology in environmental science' (Wiley-VCH, Weinheim, Germany, 2018), pp. 209–292
- [14] Gaya U.I.: 'Heterogeneous photocatalysis using inorganic semiconductor solids' (Springer Science & Business Media, Berlin, Germany, 2013)
- [15] Koohestani H.: 'Photocatalytic performance of copper oxides rod-shaped prepared by spin coating', *Micro Nano Lett.*, 2019, **14**, (1), pp. 339–343, doi: 10.1049/mnl.2018.5447
- [16] Kamegawa T., Kido R., Yamahana D.: 'Design of TiO₂-zeolite composites with enhanced photocatalytic performances under irradiation of UV and visible light', *Microporous Mesoporous Mater.*, 2013, **165**, pp. 142–147
- [17] Sacco O., Vaiano V., Matarangolo M.: 'ZnO supported on zeolite pellets as efficient catalytic system for the removal of caffeine by adsorption and photocatalysis', *Separation Purif. Technol.*, 2018, **193**, pp. 303–310
- [18] Liu S., Lim M., Amal R.: 'TiO₂-coated natural zeolite: rapid humic acid adsorption and effective photocatalytic regeneration', *Chem. Eng. Sci.*, 2014, **105**, pp. 46–52
- [19] Koohestani H.: 'Photocatalytic removal of cyanide and Cr(IV) from wastewater in the presence of each other by using TiO₂/UV', *Micro Nano Lett.*, 2019, **14**, (1), pp. 45–50
- [20] Shih Y.H., Tso C.P., Tung L.Y.: 'Rapid degradation of methyl orange with nanoscale zero valent iron particles', *Nanotechnology*, 2010, **7**, pp. 16–17
- [21] Chica A.: 'Zeolites: promised materials for the sustainable production of hydrogen', *ISRN Chem. Eng.*, 2013, **2013**, pp. 1–19
- [22] Koohestani H., Sadmezhzaad S.K., Kheilnejad A.: 'Investigation of photocatalytic performance of TiO₂ network and fiber geometries', *Desalination Water Treat.*, 2016, **57**, (50), pp. 23644–23650